P9.1 Tornado Identification Using a Neuro-fuzzy Approach to Integrate Shear and Spectral Signatures

Yadong Wang*, Tian-You Yu, Mark Yeary
School of Electrical and Computer Engineering,University of Oklahoma
Alan M. Shapiro
School of Meteorology, University of Oklahoma
Shamim Nemati
Department of Mathematics, University of Oklahoma
Michael Foster, and David L. Andra, Jr.
National Weather Service, Norman, Oklahoma

1. Introduction

Traditional tornado identification is primarily dependent on reflectivity and/or shear signatures. The detection of potential tornadic storms by identifying hook echoes was documented by Stout and Huff (1953), and was realized as a tornado precursory signature after the Illinois tornado (Fujita 1958). The NSSL Tornado Detection Algorithm (NSSL TDA) (Mitchell et al. 1998) searches for strong and localized azimuthal shears. However, if a tornado is located at far ranges or if the tornado is small compared to the radar resolution volume, the shear signature becomes difficult to identify (Brown and Lemon 1976). Recently, a half-degree angular sampling was proposed to improve the shear signatures (Brown et al. 2002). However, the statistical error of the spectral moment estimates increases due to that fewer samples are used. Because tornado debris consists of an assemble of particles of various sizes and irregular shapes, some of them have distinct polarimetric signatures that are different from hydrometers, and can be used to improve tornado detection (Ryzhkov et al. 2005).

The Doppler spectra from a tornadic region are different from Gaussian-like spectra from by other regions of the storm. Broad and flat tornado spectral signatures were found in simulated data, and bimodal spectra were observed by pulse Doppler radar (Zrnić and Doviak 1975). These distinct spectral signatures can be used to improve the detection capability.

In this work, a neuro-fuzzy method is developed based on spectral analysis, neural network and fuzzy logic, in which tornado signatures in both velocity and spectrum domains are integrated to improve the tornado detection.

*Corresponding author address: Yadong Wang, 202 W.Boyd,School of Electrical and Computer Engineering, University of Oklahoma, Norman, Oklahoma 73019 Email: wyd@ou.edu

This paper is organized as follows: in section 2, tornado spectral analysis of simulation and real data are examined and the parameters used in the neuro-fuzzy method are described; in section 3, the neuro-fuzzy tornado detection algorithm (NFTDA) is presented; its application to real tornado cases is presented in section 4; A summary and conclusions are given in section 5.

2. Tornado spectral signatures

A wide and bimodal tornado spectrum was simulated by a combined Rankine vortex model with uniform and hollow reflectivity profiles (Zrnić and Doviak 1975), similar spectra were observed by a pulse-Doppler radar (Zrnić et al. 1985). The spectrum width, σ_v, is an intuitive parameter to describe the broad spectrum feature. However, spectrum width does not provide sufficient information of the spectrum shape. Therefore other parameters are developed to characterize the tornado spectral signatures (TSS). First of all, the third order spectrum (termed bispectrum) retains the phase information of the Fourier coefficients, in which most shape information of the signal resides (Oppenheim and Lim 1981). To use the bispectrum effectively, the phase of radial integrated bispectrum (PRIB), denoted by P value (Chandran and Elgar 1993) is proposed to characterize TSS, in which the spectrum in decibel is considered as a 1D image (Yu et al. 2006). Secondly, the spectrum variance, σ_s, is used to define the flatness of a spectrum (Yu et al. 2006). Another parameter, the eigen-ratio, χ_R, defined as the ratio of the minimum to the maximum eigen values, is also included (Yeary et al. 2006).

To study how these four TSS parameters vary with range for different conditions, numerical simulations are firstly conducted. A tornado modeled by a Rankine vortex

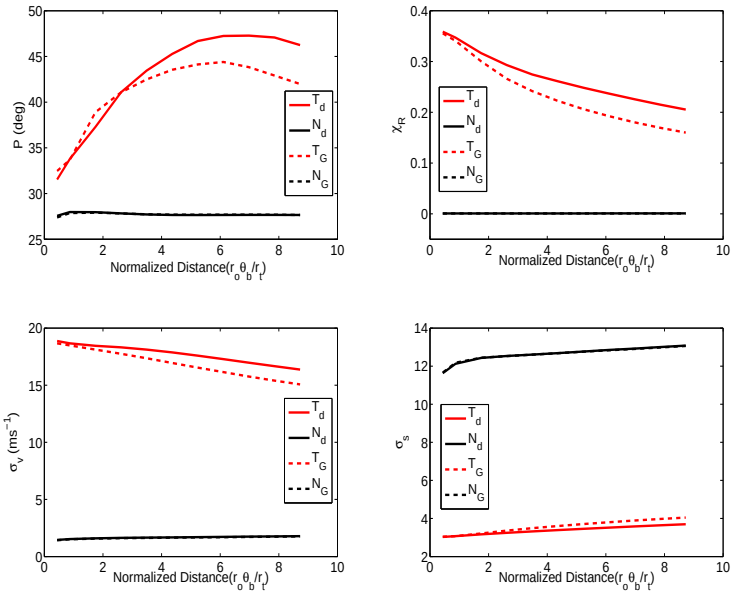

Figure 1: The variation of TSS with normalized range P value (upper left), eigen-ratio (upper right), spectrum width (lower left), spectrum variance(lower right) for tornado and non-tornado case.

within a mesocyclone is generated. The radius of the tornado is 70 m, with the maximum tangential velocity of 50 m s^{-1} and the maximum radial velocity of 15 m s^{-1}. Azimuth shear dv/dx = 0.08 s^{-1} is included. Maximum ambiguous velocity and angular sampling are 35 m s^{-1} and 1 ^{o}, respectively. Because the spectrum shape depends on the vortex location within the radar volume (Zrnić and Doviak 1975), spectra from 5 different relative azimuth angles, -0.5 ^{o}, -0.25 ^{o}, 0 ^{o}, 0.25 ^{o}, 0.5 ^{o} and 5 different ranges -125 m, -65 m, 0 m, 65 m, and 125 m are generated. In addition, both Gaussian and doughnut-shape reflectivity are simulated, and a uniform signal-to-noise ratio (SNR) of 30 dB was applied to all the data. Note only spectra from the region close to the tornado center have distinct TSS. Spectra from regions further from the vortex center are similar to those with typical Gaussian shapes. In Figure 1, T$_d$, N$_d$ represents spectra from the range cells where the tornado is centered and 5 km east of the tornado center, respectively. The subscripts d and G indicate the doughnut-shape and Gaussian reflectivity, respectively. It is apparent that distinct differences between tornado case and non-tornado case can be observed from all four parameters. These parameters are slightly effected by the reflectivity structure, and can be used to identify tornadic evens at far ranges.

Furthermore, two tornado cases, the 8 May 2003 Moore tornado, and the 10 May 2003 Edmond tornado, are used in the histogram in Figure 2. In these histograms, the regions within the damage path and with large velocity difference between adjacent azimuths (larger than 50 m s^{-1}) are defined as tornado cases, others are defined as non-tornado cases. It is evident that for tornado case, the σ_v, χ_R, and P value are large but the σ_s is small.

3. NFTDA

3a. *Motivation*

The fuzzy logic has inherit advantages for tornado detection. As exemplified in Figure 2. it is evident that there is no clear distinction between the PDF of tornado and non-tornado cases. Therefore, it is difficult to accurately set a threshold for detection. On the other hand, the fuzzy logic approach can avoid strict individual thresholds, and instead different fuzzy membership functions are used. Moreover, decision is made based on all the available parameters, which can mitigate the dependency on single parameter. As a result, more reliable and robust detection result can be obtained.

The fuzzy membership functions are initialized based on the statistical analysis of the real data. A neural network is also integrated into the fuzzy logic system. Due to the self-learning ability of neural networks, the membership functions will be adjusted through the training process (Wang et al. 2005).

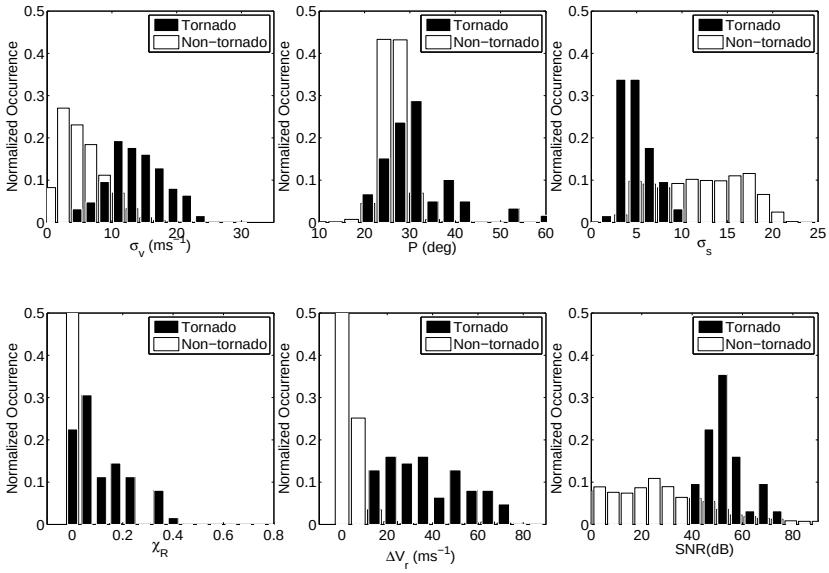

Figure 2: Normalized histogram of spectrum width (upper left), P value (upper middle), spectrum variance (upper right), eigen-ratio (lower right), velocity difference (lower middle), signal to noise ratio (lower right) for tornado and non-tornado regions.

3b. *Neuro-fuzzy logic in tornado detection*

The fuzzy logic system consists of four subsystems: fuzzification, rule inference, aggregation, and defuzzification (Liu and Chandrasekar 2000). A schematic diagram of the neuro-fuzzy system is shown in Figure 3.

In fuzzification, two membership functions, S-shape and Z-shape, are used in this work to convert crisp inputs into fuzzy membership degrees. These two functions, representing tornado and non-tornado cases for all the parameters, are shown in Figure 4. In the rule inference, the correlation-product, which is commonly used in the multi-input and multi-output fuzzy system, is used to establish the relationship between a fuzzy input and output. The two final degrees will be the inputs of another node termed aggregation. In this node, a maximum operation will be performed to make the final decision, and a detection result will be given in the defuzzification part.

4. Performance evaluation

The performance of the NFTDA is evaluated using radar data from two tornado events: 1.) 10 May 2003 Edmond OK F3 tornado 2.) 8 May 2003 Moore OK F4 tornado. Detection results and tornado damage paths from ground survey for these two events are shown in Figure 5. Additionally NSSL TDA on KOUN and NWS TDA on KTLX are denoted by triangles and downward triangles, respectively, and are termed TDA-KOUN and TDA-KTLX. Results from the NFTDA on KOUN is denoted by solid circles. The damage path with green shade represents 8 May case, and cyan shade represents 10 May case. The location of KTLX is marked, and KOUN is located at the origin.

4a. *The tornado event on 10 May 2003 Edmond OK*

The tornado with maximum intensity of F3 occurred 7 miles south of Edmond, Oklahoma on 10 May 2003. This tornado lasted approximate 37 minutes and moved 18 miles. The time series data were collected by KOUN for approximately two hours. At the same time the TWIN LAKES (KTLX) operational WSR-88D, which is 20 miles northeast of the KOUN, also observed the tornado and recorded the level II data. KTLX locates closer to tornado compared to KOUN, thus the NWS TDA detection results are used as reference. A comparison of detection results are shown in Tables 1, 2 and 3.

At 0331, 0343, 0349, and 0355 UTC, the tornado locations detected by the TDA-KOUN were within the damage path. However, at 0337 a tornado was identified approximately 2 km north of the damage path. In addition, two locations at approximately 6 km north and south of the damage path were identified as tornado at 0401 UTC. After 0401 UTC no tornado was detected, although the tornado damage path suggested the tornado existed beyond that time.

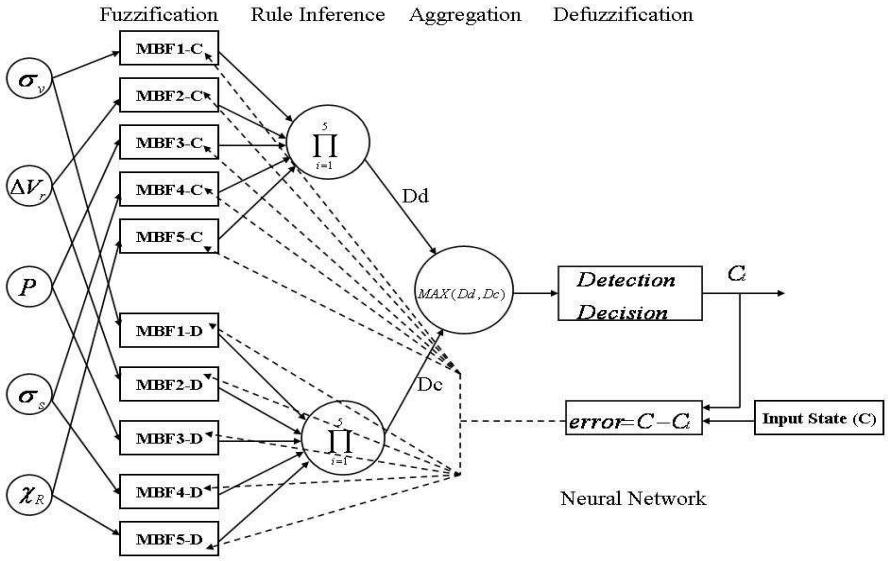

Figure 3: The flow chart of the neuro-fuzzy tornado detection algorithm (NFTDA).

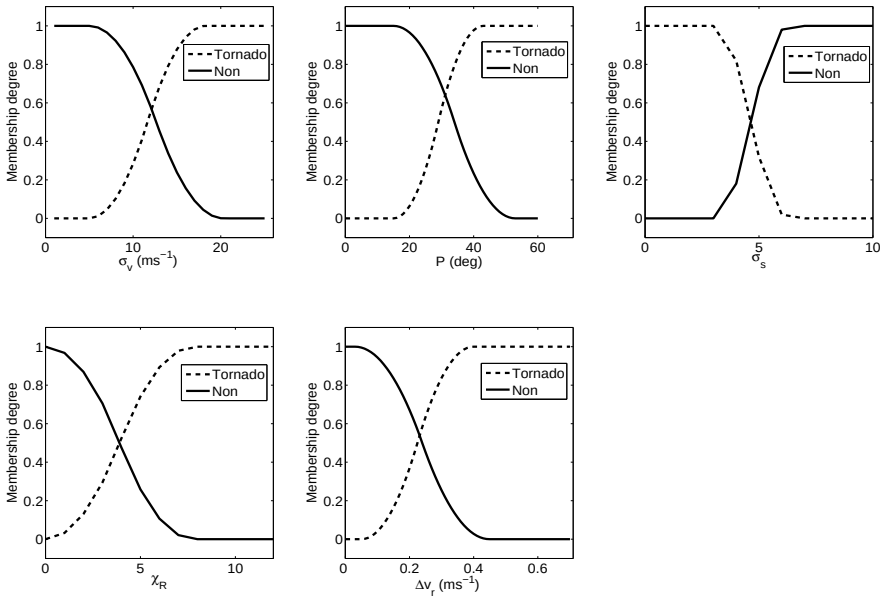

Figure 4: Membership functions used in the NFTDA for: spectrum width (upper left), P (upper middle), spectrum variance (upper right),, eigen-ratio (lower right), velocity difference (lower middle).

Table 1: Detection results from NFTDA

Time(UTC)	03:31	03:37	03:43	03:49	03:55	04:01	04:07	04:13	04:19
Range(km)	35.625	37.625	39.625	40.625	42.625	44.125	48.125	52.625	55.375
Detection Results	Yes	Yes	Yes	Yes	Yes	No	Yes	Yes	Yes
Match Results	Yes	Yes	Yes	Yes	Yes	N/A	Yes	Yes	Yes

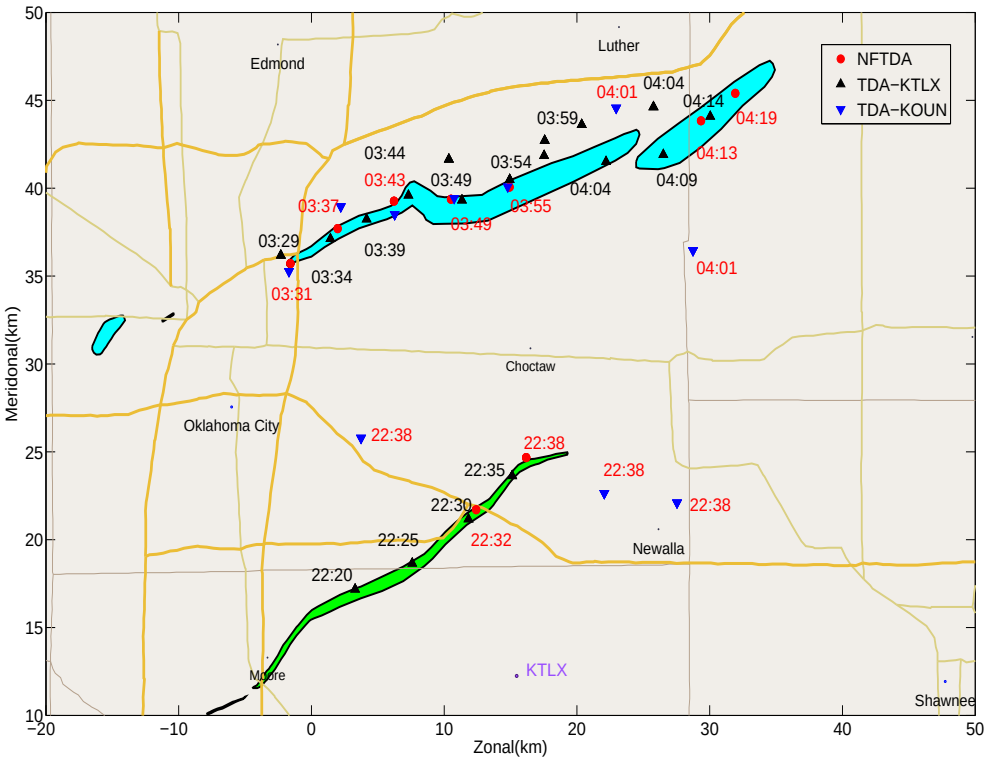

Figure 5: Detection results from three tornado detection algorithms: TDA-KTLX, TDA-KOUN, NFTDA

Table 2: Detection results from TDA-KOUN

Time(UTC)	03:31	03:37	03:43	03:49	03:55	04:01	04:07	04:13	04:19
Range(km)	35.188	38.892	38.892	40.744	42.596	46.33/33.36	N/A	N/A	N/A
Detection Results	Yes	Yes	Yes	Yes	Yes	Yes	No	No	No
Match Results	Yes	Yes	Yes	Yes	Yes	No	No	No	No

Table 3: Detection results from TDA-KTLX

Time(UTC)	03:29	03:39	03:44	03:49	03:54	03:59	04:04
Range(km)	27.36	25.75	25.75	25.75/27.36	25.75/27.36	27.36/28.97	27.36/30.40
Detection Results	Yes	Yes	Yes	Yes	Yes	Yes	Yes
Match Results	Yes	Yes	Yes	Yes/No	Yes/No	No/No	Yes/No

Time(UTC)	04:09	04:14	04:19
Range(km)	28.97	30.58	32.16
Detection Results	Yes	Yes	Yes
Match Results	Yes	Yes	Yes

The detection results from the NFTDA and TDA-KOUN are similar from 0331 UTC to 0355 UTC. The distance between the tornado and KOUN varies approximately from 35.625 km to 42.625 km during this period. At later times (0407, 0413 and 0419 UTC) when the tornado moved further away from the KOUN, the NFTDA could still detect the tornado while the TDA-KOUN did not identify the tornado. It is evident that the NFTDA detection results agree with the damage path more favorably than the results from the TDA-KOUN.

4b. *The tornado event on 8 May 2003 Moore OK*

On 8 May 2003, a maximum intensity of F4 tornado was observed by KOUN, which lasted about 23 minutes and moved approximately 14 miles. Both KOUN and KTLX recorded the detection results of this tornado event, which are showed in Figure 5. However only limited KOUN time series data (at 2232 and 2238 UTC) are available. Large azimuth shear were observed in some locations due to second-trip echoes. The NFTDA can suppress the shear information to reduce the false detections in these regions.

5. Summary and conclusions

In this paper a new tornado detection algorithm NFTDA which uses fuzzy logic and neuro network is presented. Besides velocity shear, additional parameters describing spectral signatures, σ_v, P, χ_R and σ_s, are used in the NFTDA. All these four parameters show the significant differences between tornado case and non-tornado case even in far range. Two tornado events are used to evaluate the performance of the NFTDA. Compared to traditional shear-based TDA, the NFTDA is less sensitive to the velocity smoothening effect and is able to detect tornadoes in far range. In addition extending the detection range, this NFTDA can also decrease the false alarm rates caused by second-trip echoes.

6. ACKNOWLEDGMENTS

This work is supported by NOAA CSTAR program through the funding NA17RJ1227. The authors thank NSSL's support for collecting the time series data on KOUN, E. Forren and M. Jain at NSSL for providing KOUN TDA results, and also thank Jennifer Palucki from School of Meteorology, University of Oklahoma providing the damage path.

References

Brown, R. A. and Lemon, L. R. (1976). Single Doppler radar vortex recognition. part ii: Tornadic vortex signatures. *Prepr. Radar Meteor. Conf.*, pages 104–109.

Brown, R. A., Wood, V. T., and Sirmans, D. (2002). Improved tornadoes detection using simulated and actual WSR-88D data with enhanced resolution. *J. Atmos. Oceanic Technol.*, 19:1759–1771.

Chandran, V. and Elgar, S. L. (1993). Pattern recognition using invariants defined from high order spectra-one-dimensional inputs. *IEEE Trans. Signal Processing*, 41:205–212.

Fujita, T. (1958). Mesoanalysis of the illinois tornadoes of 9 april 1953. *J. Atmos. Sci.*, 15:288–296.

Liu, H. and Chandrasekar, V. (2000). Classification of hydrometeors based on polarimetric radar measurements: Development of fuzzy logic and neuro-fussy system, and in-situ verification. *J. Atmos. Oceanic Technol.*, 17:140–164.

Mitchell, E. D., Vasiloff, S. V., Stumpf, G. J., Witt, A., Eilts, M. D., Johnson, J. T., and Thomas, K. W. (1998). The National Severe Storms Laboratory tornado detection algorithm. *Wea. Forecasting*, 13:352–366.

Oppenheim, A. V. and Lim, J. S. (1981). The importantance of phase in signals. *Proc. IEEE*, 69:529–541.

Ryzhkov, A. V., Schuur, T. J., Burgess, D. W., and Zrnic, D. S. (2005). Polarimetric tornado detection. *J. Appl. Meteorol.*, 44:557–570.

Stout, G. E. and Huff, F. A. (1953). Radar records illinois tornadogenesis. *Bull. Amer. Meteor. Soc.*, 34:281–284.

Wang, Y., Yu, T.-Y., Yeary, M., Shapiro, A., Zrnić, D., Foster, M., and D. L. Andra, J. (2005). Tornado detection using a neural-fuzzy method. *32nd Conf. on Radar Meteor.*

Yeary, M., Nemati, S., Yu, T.-Y., and Wang, Y. (2006). Tornadic time series detection using eigen analysis and a machine intelligence-based approach. *IEEE Trans. Geosci. Remote Sens.*, under review.

Yu, T.-Y., Wang, Y., Shapiro, A., Yeary, M., Zrnic, D. S., and Doviak, R. J. (2006). Characterization of tornado spectral signatures using higher order spectra. *J. Atmos. Oceanic Technol.*, in preparation.

Zrnić, D. S., Burgess, D. W., and Hennington, L. D. (1985). Doppler spectra and estimated windspeed of a violent tornado. *J. Climate Appl. Meteor.*, 24:1068–1081.

Zrnić, D. S. and Doviak, R. J. (1975). Velocity spectra of vortices scanned with a pulsed-Doppler radar. *J. Appl. Meteorol.*, 14:1531–1539.